Diseases **2014**, *2*, 148-167; doi:10.3390/diseases2020148

OPEN ACCESS

diseases

ISSN 2079-9721

www.mdpi.com/journal/diseases/

Article

NF-κB Activation Exacerbates, but Is not Required for Murine Bmpr2-Related Pulmonary Hypertension

Megha Talati [1,†], Haitham Mutlak [2,†], Kirk B. Lane [1], Wei Han [1], Anna Hemnes [1], Outi Mutlak [3], Tom Blackwell [1], Rinat Zaynagetdinov [1], Timothy S. Blackwell [1] and James West [1,*]

[1] Division of Allergy, Pulmonary, and Critical Care Medicine, Vanderbilt University Medical Center, Nashville, TN 37232, USA; E-Mails: Megha.Talati@vanderbilt.edu (M.T.); Kbondlane@gmail.com (K.B.L.); wei.han@vanderbilt.edu (W.H.); anna.r.hemnes@vanderbilt.edu (A.H.); tom.blackwell@vanderbilt.edu (T.B.); rinat.z.zaynagetdinov@vanderbilt.edu (R.Z.); timothy.blackwell@vanderbilt.edu (T.S.B.)

[2] Department of Anesthesiology, Intensive Care Medicine and Pain Therapy, University Hospital Johann Wolfgang Goethe, Frankfurt 60590, Germany; E-Mail: haitham.mutlak@kgu.de

[3] Department of Anesthesiology, University of Colorado Health Sciences Center, Denver, CO 80045, USA; E-Mail: outi.mutlak@googlemail.com

† These authors contributed equally to this work.

* Author to whom correspondence should be addressed; E-Mail: j.west@vanderbilt.edu; Tel.: +615-343-0895; Fax: +615-343-3480.

Received: 18 April 2014; in revised form: 20 May 2014 / Accepted: 21 May 2014 / Published: 30 May 2014

Abstract: Aim: The present study investigates the role of NF-κB in Bmpr2-related pulmonary hypertension (PH) using a murine model of PH with inducible overexpression of a cytoplasmic tail Bmpr2 mutation. Methods and Results: Electrophoretic mobility shift assay for nuclear extracts in $Bmpr2^{R899X}$ mouse lung and immunohistochemistry for NF-κB p65 in human PAH lung demonstrate that NF-κB is activated in end-stage disease. Acute inflammation or expression of a constitutively active NF-κB elicits a strong suppression of the BMP pathway in mice inversely correlating to activation of NF-κB targets. However, Bmpr2 mutation does not result in NF-κB activation in early disease development as assessed by luciferase reporter mice. Moreover, Bmpr2 mutant mice in which NF-κB activation is genetically blocked develop PH indistinguishable from that without the block. Finally, delivery of a virus causing NF-κB activation strongly exacerbates development of PH in Bmpr2 mutant mice, associated with increased remodeling.

Conclusion: NF-κB activation exacerbates, but is not required for Bmpr2-related PH. Pulmonary vascular-specific activation of NF-κB may be a "second hit" that drives penetrance in heritable PH.

Keywords: pulmonary arterial hypertension; bone morphogenic protein receptor type 2; NF-κB; inflammation

1. Introduction

Pulmonary arterial hypertension (PAH), in animal models and probably in human patients, can derive from many primary insults. These include hypoxia (perhaps modeling human diseases such as COPD) [1], primary defects in vasoreactivity (perhaps modeling calcium-channel responsive human PAH patients) [2], metabolic problems (as in fawn-hooded rats) [3], proliferative problems (likely the defect in lymphangioleiomyomatosis) [4], and inflammation (as in schistosomiasis-related PAH, and probably sarcoidosis) [5]. From end-stage pathology and symptomology in patients, it is not clear which of these, if any, is the mechanism behind Group I PAH, the idiopathic and heritable forms.

The majority of heritable PAH is associated with mutations in BMPR2 [6,7]. In the non heritable idiopathic form, even when BMPR2 is not mutated, it is suppressed, and the downstream molecular consequences are indistinguishable from mutated BMPR2 [8]. Mice with transgenic overexpression of Bmpr2 develop a form of PH which in many cases is associated with recruitment of inflammatory cells and increased expression of multiple cytokines [9–12]: in cell culture there is a clear negative feedback loop between the BMP pathway and cytokine expression [13]. Moreover, it has been hypothesized for decades that idiopathic PAH may be a primarily inflammatory disease [14], supported by numerous current lines of research [15–18].

Perhaps the most central pathway in the regulation of inflammation is NF-κB [19]. The NF-κB complex is normally inhibited in the cytoplasm through binding to IκB. IκB is degraded as a result of inflammatory signaling, allowing NF-κB complex components including RelA and p50 to enter the nucleus and initiate transcription.

The goal of the current project was to determine whether NF-κB activation is involved in the development of Bmpr2-related PH. We tested whether Bmpr2 mutation results in NF-κB activation *in vivo* using a triple-transgenic cross to an NF-κB luciferase reporter mouse line; we tested whether NF-κB activation was required for the development of Bmpr2-related PH using a triple-transgenic cross to a dominant negative IB line, and we tested whether NF-κB activation would increase disease penetrance in Bmpr2 mutant mice using a dominant RelA virus.

For all of these studies we used mice with doxycycline inducible universal expression of a dominantly acting Bmpr2 mutation, R899X [20]. These mice are allowed to grow to adulthood before activating their mutation, to avoid developmental defects. The R899X mutation is a truncation mutation in the cytoplasmic tail domain of Bmpr2, which leaves canonical SMAD signaling intact [10], but which directly interacts with and modulates the activity of SRC, LIMK1, and TCTEX1 [21]. Cytoplasmic tail domain mutations are common in heritable PAH patients [22], and because they do not impact as many

pathways as ligand binding or kinase domain mutations are used here as a sort of "least common denominator" for BMPR2 mutations.

2. Experimental Section

2.1. Electrophoretic Mobility Shift Assay (EMSA)

Snap frozen whole lung from Rosa26-only control mice or Rosa26-Bmpr2^{R899X} mice shown to have elevated RVSP in prior studies [20] were prepared for nuclear extracts. EMSA for NF-κB binding activity were done as previously described [23]. A double-stranded oligonucleotide probe, containing consensus NF-κB motif (Stratagene, La Jolla, CA, USA) was used in these studies. For supershift studies, p50 antibody (Santa Cruz cat Sc-114) was added during incubation of nuclear extract with binding buffer on ice for 30 min, before incubation with labeled oligonucleotides.

2.2. IP Lipopolysaccharide (LPS)

A stock solution of LPS derived from E. coli serotype 0111:B4 (Sigma-Aldrich) dissolved in PBS was stored in small aliquots at −20 °C. Immediately before each experiment, an aliquot of LPS was thawed, sonicated, and diluted in PBS yielding a final concentration of 1 mg/mL. Mice in the LPS-Group received 5 mg/kg LPS intraperitoneally (IP) (100 μL–125 μL). Control mice received the same amount of sterile saline IP. 6, 12 and 24 h after LPS administration a lethal dose of pentobarbital was injected. Immediately after a surgical level of anesthesia was achieved, the chest wall was opened, the left atria nicked, and the animal euthanized through injection of PBS (2 mL) into the right ventricle to remove all pulmonary intravascular blood. Lungs were divided and processed for molecular studies. These animal experiments were approved by the University of Colorado Intramural Animal Care and Use Committee.

2.3. Western Blotting

Tissues were homogenized in 500 μL of RIPA Buffer (PBS, 1% ipegal, 0.5% sodium deoxycholate, 0.1% SDS) with protease and phosphatase inhibitor cocktail (Sigma-Aldrich, St. Louis, MO, USA). Tissues were centrifuged at 4 °C (15 min, 15,000 × *g*) and protein concentration was determined by Bradford microassay (Bio-Rad, Hercules, CA, USA) on the supernatant. Equal amounts of protein extracts were denatured at 95 °C in a denaturing sample buffer. Protein from each sample (15–70 μg) was separated by electrophoresis in a 10% or 8%–16% Tris-Glycine gel and transferred onto a PVDF membrane. The membrane was blocked for 45 min at room temperature with phosphate-buffered saline containing 5% non-fat dry milk and 0.05% Tween-20 and probed overnight at 4 °C with primary rabbit polyclonal antibody against Id1 (1:200 Dilution, Santa Cruz Biotechnology, Santa Cruz, CA, USA), pSMAD1/5/8 and SMAD 1 (1:200 dilution, Cell Signaling Technology, Danvers, MA, USA) and β-actin (1:1,000, Abcam, Cambridge, MA, USA). The membrane was then incubated at 37 °C for 45 min with horseradish peroxidase-labeled donkey anti-mouse immunoglobulin secondary antibody (1:1,000 dilution, Santa Cruz Biotechnology, Santa Cruz, CA, USA). Horseradish peroxidase was detected using the ECL+ Western blotting detection system (Amersham Biosciences, Piscataway, NJ, USA). Densitometry was performed using ImageJ (public domain software published by the NIH).

2.4. Quantitative RT-PCR

RNA was made using an RNEasy mini kit (Qiagen, Valencia, CA, USA), and first strand cDNA was made using 1 μg total RNA using a QuantiTect® Reverse Transcription Kit (Qiagen, Valencia, CA, USA). Quantitative real-time PCR was performed using a total reaction volume of 25 μL, containing 5 μL of diluted cDNA, 12.5 μL iTaq SYBR Green Supermix with ROX (BioRad Laboratories, Hercules, CA, USA) and 0.78 μL of each oligonucleotide primer. Primer sequences were as follows: BMP4 (TAGCAAGAGTGCCGTCATTCC, ACCAGTGCTGTGGATCTGCTC), Grem2 (TTACAAGGACGGCAGCAGC, GCGTCTTGCACCAGTCACTC), Il1b (CGTGGACCTTCC AGGATGAG, AATGGGAACGTCACACACCAG), HPRT (TGCTCGAGATGTCATGAAGGAG, TTTAATGTAATCCAGCAGGTCAGC). HPRT expression was used for normalization.

2.5. Luciferase Assays

HLL mice are a previously described NF-B reporter strain that express luciferase under the control of an NF-B dependent promoter [24]. These were bred to Rosa26-Bmpr2^{R899X} mice to make Rosa26/HLL or Rosa26-Bmpr2^{R899X}/HLL double and triple transgenic mice. Adult mice were fed doxycycline in chow, then NF-B -dependent luciferase activity measured as previously described [25] on day 1, and week 1, 2, and 3 in live mice. Briefly, mice are anesthetized, have chest and abdomen shaved, are injected with Luciferin, and imaged under an intensified charge-coupled device. This is a survival procedure: the same mice are used at each time point. After week 3, mice received 5 mg/kg LPS IP, and were measured at 6 h, 1 day, 2 days, and 3 days. Mice had returned to baseline by the end of 3 days. At the end of week 4, mice were sacrificed, and organs collected for measurement of luciferase activity across tissues as previously described [25]. All animal procedures were approved by the Vanderbilt IACUC.

2.6. Echocardiography and Hemodynamic Phenotyping

Two-dimensional echocardiography was performed using Vivo 770© High-Resolution Image System (VisualSonics© Toronto, ON, Canada). Echocardiograms including B-mode, M-mode and spectral Doppler images were obtained the day prior to sacrifice under isoflurane anesthetic. Velocity time integral and heart rate were measured in the ascending aorta, diameter measured in the same location. Stroke volume [SV(calc)] was derived using the formula SV = {[π (Aortic diameter)2/4] * [Aortic velocity time integral]}. Cardiac output was [CO (calc)] derived using formula CO = SV(calc) * heart rate (HR) [26,27].

Hemodynamic phenotyping was performed as previously described [10,20]. Briefly, mice are anesthetized with tribromoethanol, systemic pressure checked by tail cuff, and then undergo closed-chested intrajugular right cardiac catheterization.

Pulmonary vascular resistance (PVR) was calculated based on an approximation of the standard formulation of 80 * (mean PA pressure − mean pa wedge)/cardiac output, where mean PA pressure is calculated using RV pressures rather than PA pressures and setting wedge pressure to zero (both of which are unobtainable in mice). Mean PA pressure is calculated as (2/3) diastolic pressure + (1/3) systolic pressure, but we set diastolic pressures to zero, which would tend to underestimate PVR, to

avoid artifacts associated with changing pressures due to breathing in a closed-chested system. The final calculation is thus PVR = (80/3) * (RVSP/CO).

All animal procedures were approved by the Vanderbilt IACUC.

2.7. dnIkB Experiments

To prevent NF-κB activation, Rosa26-only or Rosa26-Bmpr2^{R899X} mice were crossed to previously reported TetO$_7$-dnIkB mice to create double or triple transgenics [10,20]. TetO$_7$-dnIκB mice express a mutant avian IB that cannot be degraded [28]. Rosa26-rtTA2 mice express the reverse tetracycline transactivator universally; when used alone these were controls. Rosa26-Bmpr2^{R899X} mice are the Rosa26-rtTA2 mice crossed to TetO7-Bmpr2^{R899X} mice, which then express the dominant negative tail domain mutation R899X in all tissue types, when transgene expression is induced with doxycycline [20]. Adult mice were given doxycycline ad libitum at 0.2 g/kg in chow to activate transgenes, and after six weeks underwent hemodynamic phenotyping as above.

2.8. RelA Virus Administration

Adult Rosa26-only or Rosa26-Bmpr2^{R899X} mice had transgene induced by 0.2 g/kg doxycycline in chow. After two weeks 1 L of 1012pfu/mL RelA virus was administered intra-trachial in 50 L of sterile PBS. Control animals received 1 L of LUC 1-5z11 in 50 L of sterile PBS. RelA and control adenovirus were created as previously described [25]. After an additional four weeks, animals underwent hemodynamic phenotyping as above.

2.9. IKTA Mice

IKTA mice (IKKβ Trans-Activated) selectively expressing a constitutively active form of human IKKβ in airway epithelium have been reported previously [29]. We used 8 week-old male IKTA mice and WT littermate controls on the original FVB background. To activate transgene expression, mice were provided ad lib with 0.5 mg/mL doxycycline (dox) in drinking water for 2 weeks. Then mice were sacrificed, lungs were perfused with PBS until free of blood by visual inspection and snap frozen in liquid nitrogen.

2.10. Morphometry

After euthanasia, the left atria were removed and the pulmonary circulation was perfused with PBS using syringe-generated flow. The left lung was inflated with 0.8% low melt agarose at constant inflation pressure and embedded in paraffin. Samples were transversely sectioned at 6 μm thickness, and immunostained with antibody against smooth muscle alpha actin (αSMA, Sigma-Aldrich, St. Louis, MO, USA) with a fluorescent (GFP) secondary, and counterstained with DAPI. Random fields were selected with DAPI, avoiding fields with large airways or bronchi, and then vessel size and muscularization measured for each vessel identified by αSMA staining. Ten fields are used per lung, and lungs from at least three mice per group are surveyed.

2.11. Statistical Methods

Statistical tests were performed using the JMP program (SAS, Cary, NC, USA). One-way or two way ANOVA were used to determine effects of interacting variables, with post-hoc Fischer's LSD used to determine difference between individual groups.

3. Results and Discussions

3.1. NF-κB Activation is Present in Human and Murine Pulmonary Hypertension

NF-κB activation has been extensively studied in the monocrotaline rat model of inflammatory PH [30], and has been recently extensively studied in human end-stage PAH [31], but we were interested in whether we saw it in our Rosa26-Bmpr2^{R899X} model. To determine whether there was evidence of NF-κB activation in our murine model of Bmpr2, we performed EMSA on flash frozen whole lung from Rosa26-Bmpr2^{R899X} or control mice. The mice used had eight weeks of transgene activation from a previous study [20], and the Bmpr2^{R899X} mutants had developed elevated right ventricular systolic pressures (RVSP).

We found that Rosa26-Bmpr2^{R899X} mice had significantly increased nuclear NF-κB compared to Rosa26-only controls (Figure 1A, left 6 lanes). Because only nuclear extracts were used, and because only active NF-κB is found in the nucleus, the darker bands in the Bmpr2^{R899X} lanes indicate increased activity. Specificity is demonstrated by elimination of bands through addition of p50 antibodies (Figure 1A, right 4 lanes). The p50 antibodies used interfere with DNA binding, resulting in disappearance of the band, rather than supershift. Immunohistochemistry for cells with nuclear RelA (indicating activation) shows isolated cells with strong nuclear staining in human idiopathic PAH (Figure 1B) similar to seen in Bmpr2-related PAH in our recent publication (42). A similar finding is presented in a recent study of NF-κB activation in human end-stage PAH [31].

3.2. The BMP Pathway is Suppressed during Acute Inflammation

The rationale for these experiments was to determine whether acute inflammation, and activation of NF-κB, resulted in modulation of the BMP pathway in live animals. The purpose of these experiments was to establish a signaling link, not as necessarily directly bearing on the etiology of PAH.

To determine whether there was evidence for a role for the BMP pathway in regulating inflammation *in vivo*, we treated wild-type mice with IP LPS, and sacrificed four mice each at 6, 12, and 24 h, compared to controls. We found that at the 6 h time point, at the peak of inflammation [32], there was almost complete abrogation of BMP signaling, as assessed by Smad1/5/8 phosphorylation (Figure 2A). Protein expression of canonical Smad1 target Id1 is suppressed at both 6 and 12 h (Figure 2B). Quantitative RT-PCR for expression of BMP pathway components found no change in Bmpr2 expression (not shown), but a greater than tenfold downregulation of Bmp4 at 6 h, strongly inversely correlated to canonical NF-κB target Il1β, coupled with a long-term decrease in secreted BMP inhibitor Grem2 (PRDC) (Figure 2C). One explanation for this decrease in Grem2, which reaches a minimum at the timepoint associated with return of pSmad activation, is that it is

counter-regulatory: NF-κB activation results in suppression of BMP signaling, as well as suppression of BMP inhibitor Grem2, with the result that this suppression is, in normal mice, temporary.

Figure 1. NF-κB activation is present in pulmonary arterial hypertension. (**A**, **left**) Electrophoretic Mobility Shift Assay (EMSA) using lung nuclear protein extracts from Rosa26-only (control) or Rosa26-Bmpr2^{R899X} mice with elevated right ventricular systolic pressures (RVSP). Two NF-κB bands composed of RelA/p50 heterodimers and p50 homodimers are identified. Each lane is the result from a separate mouse. White space indicates non-adjacent lanes, but identically processed and from the same blot. (**A**, **right**) The rightmost four lanes demonstrate specificity of the EMSA bands using p50 antibodies to eliminate the p50 bands. (**B**) Lung from control (**left**), idiopathic PAH (IPAH), and heritable PAH (HPAH) (42) patients shows that the latter conditions are associated with increased NF-κB and increased nuclear localization (red) in some cells.

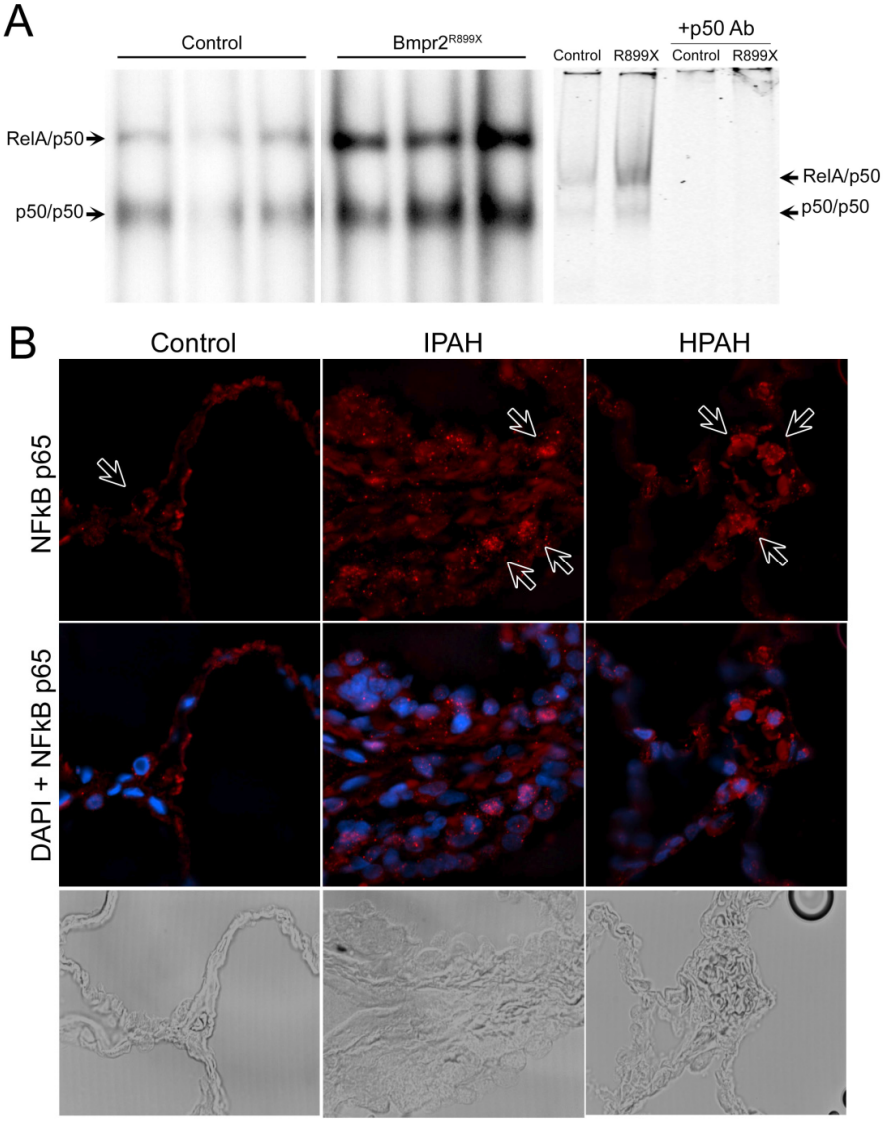

To determine specificity of effect, we measured protein levels of Smad1 target Id1 in whole lung from mice with doxycycline-inducible expression of IKTA, a constitutively active form of human IKKβ, resulting in constitutive NF-κB activation. We found on average 3× suppression of Id1 in IKTA

mouse lung (Figure 2D), suggesting that it is NF-κB, not other consequences of LPS, that suppresses BMP pathway activity.

Figure 2. BMP pathway activity is transiently suppressed during LPS-induced lung injury. (**A**) Smad1/5/8 phosphorylation is almost completely abolished at six hours after 5 mg/kg IP LPS. (**B**) Canonical Smad1 target Id1 is greatly reduced at 6 and 12 h after 5 mg/kg IP LPS. (**C**) Expression of BMP4 in whole mouse lung is strongly suppressed at six hours, partially recovering at 12 and 24 h (p = 0.0003 by ANOVA, p = 0.0037 by Wilcoxon); expression of secreted BMP pathway inhibitor Grem2 remains suppressed throughout (p = 0.0005 by ANOVA, p = 0.0090 by Wilcoxon). Canonical NF-κB target Il1 expression correlates inversely (−0.8) with BMP4 expression. N = 4 mice per time point. (**D**) Canonical Smad1 target Id1 is reduced roughly threefold in lungs from mice engineered to have constitutive activation of NF-κB, as determined by densitometry (plotted below western blot, with Id1 protein normalized to beta actin), p = 0.012 by ANOVA/p = 0.06 by signed rank (nonparametric test).

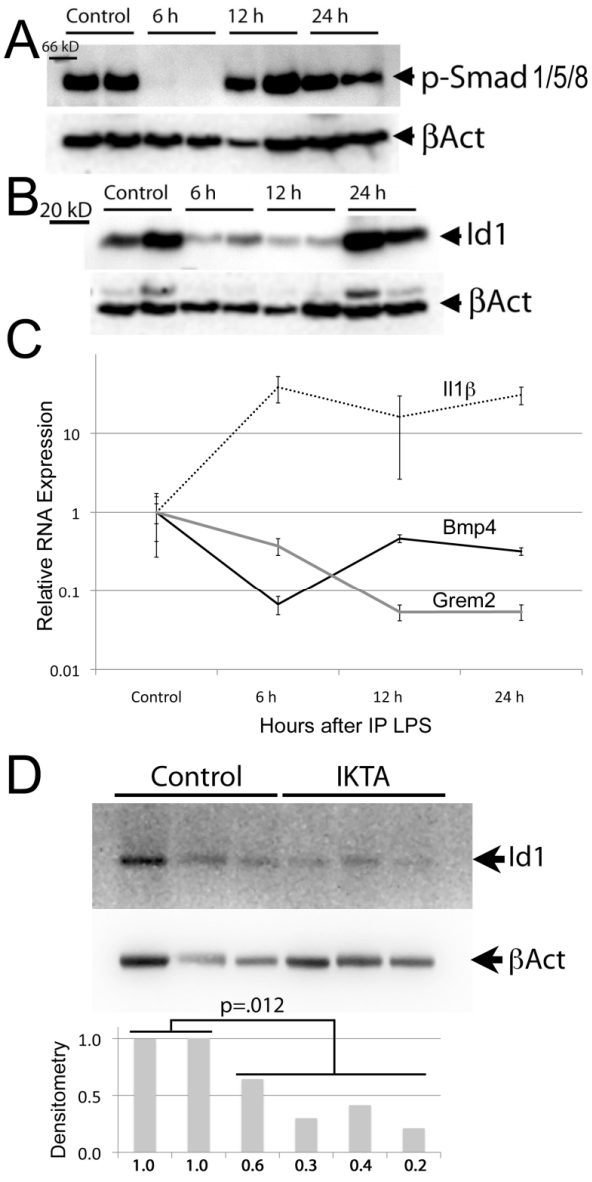

3.3. Expression of the Bmpr2^{R899X} Transgene Suppresses Basal NF-κB Activation

The rationale for these experiments was to determine whether induction of disease-causing Bmpr2 mutation resulted in modulation of NF-κB *in vivo*. Based on the late stage NF-κB activation seen in Figure 1, and on the apparently reciprocal relationship between inflammation and BMP expression suggested by Figure 2, we hypothesized that expression of the Bmpr2^{R899X} transgene would result in NF-κB activation at early time points.

HLL mice express luciferase under the control of an NF-κB dependent promoter [24]. To determine whether activation of the Bmpr2^{R899X} transgene was pro-inflammatory, we created triple-transgenic Rosa26-rtTA2M2 X TetO$_7$-Bmpr2^{R899X} X HLL mice, or Rosa26-rtTA2M2 X HLL double transgenic mice as controls. Adult mice were fed doxycycline for three weeks, with NF-κB activity assessed the day after induction, and weekly for three weeks. After three weeks, mice received IP LPS, and NF-κB activity assessed at 6 h, 1 day, 2 days, and 3 days. At seven days post-LPS, mice were sacrificed and organs removed to determine organ-specific NF-κB activity. The overall time course was intended to capture mice prior to the development of elevated RVSP, which might increase NF-κB activity for mechanical reasons.

We found that in measuring luciferase activity over the abdomen, Bmpr2^{R899X} mice had roughly half the NF-κB activity of controls, and this was stable over time (Figure 3A). However, Bmpr2^{R899X} mice were equally capable of responding to an acute inflammatory event (IP LPS injection). In measuring luciferase over the chest, Bmpr2^{R899X} mice had NF-κB activity more similar to controls (Figure 3B). Of the 10 organs assessed, NF-κB activity was reduced on average twofold in Bmpr2^{R899X} mice in six (Figure 3C), with lung being one of the exceptions. In no tissue was NF-κB activity increased. This is not a result of differential gene targeting; Bmpr2^{R899X} transgene expression is consistent across organs [20].

3.4. NF-κB Activation Is not Required for Murine Bmpr2-Related PH

In order to determine whether NF-κB activation is required for murine Bmpr2-related PH, we compared four groups of mice. All mice had Rosa26-rtTA2-M2, which produces universal expression of the rtTA2-M2 variant of the reverse tetracycline transactivator [20]. Two of the groups also had expression of the well-characterized NF-κB inhibitor transgene, dnIkB; two also had expression of our previously published dominant negative Bmpr2 transgene, R899X. Adult mice were maintained on doxycycline for six weeks to activate transgenes, and then were subjected to measurement of systemic pressure by tail cuff, closed-chested intrajugular heart catheterization, blood glucose measurement, and various morphologic measurements.

Rosa26-Bmpr2^{R899X} mice had significantly higher RVSP compared to controls, but this was not altered by expression of dnIkB (Figure 4A). The low penetrance in the Bmpr2^{R899X} mice is typical in our experience for Rosa26-Bmpr2^{R899X} not stressed by altitude, diet, age, or other factors. Non-fasting blood glucose was also higher in Bmpr2^{R899X} mice compared to controls (178 *vs.* 153 mg/dL, $p < 0.0001$ by *t*-test, $p = 0.0184$ by Wilcoxon) as previously reported [33], but this also was not affected by dnIkB. Systemic pressures were equivalent across all groups. Mice expressing the dnIkB transgene had significantly lower proportional left heart weights (by about 7%, $p = 0.02$ by *t*-test,

$p = 0.0049$ by Wilcoxon), a phenomenon previously seen with NFkB inhibition [34], implying strength of expression was sufficient to produce phenotype. Expression of the dnIkB had no effect on Smad phosphorylation (Figure 4B) or on muscularization of vessels (Figure 4C), although there was a trend to increased partially muscularized small vessels.

Figure 3. Expression of $Bmpr2^{R899X}$ transgene does not result in NF-κB activation in live mice (**A**) NF-κB activity in abdomen of live mice, assayed by transgenic luciferase-reporter construct, with or without additional $Bmpr2^{R899X}$ transgene. Taken as a whole the $Bmpr2^{R899X}$ curve is lower than the control curve at $p = 0.0006$ by ANOVA, $p = 0.0037$ v Wilcoxon rank sum prior to intraperitoneally lipopolysaccharide (IP LPS) injection but the difference disappears when LPS is injected. These are raw luciferase/unit area. $N = 4–6$ per group. (**B**) NF-κB activity in chest of live mice, assayed by transgenic luciferase-reporter construct, with or without additional $Bmpr2^{R899X}$ transgene. No individual time point is significantly different, but taken as a whole the $Bmpr2^{R899X}$ curve is lower than the control curve at $p = 0.05$. These are raw luciferase/unit area numbers, $n = 5$ per group. The first four time points (weeks 0–4) were statistically indistinguishable, and have been grouped as "base" **(C)** NF-κB activity in individual organs of $Bmpr2^{R899X}$ mice ($n = 5–6$ per organ) normalized to activity in the same organ in control mice. The majority of organs from $Bmpr2^{R899X}$ mice have significantly lower NF-κB activity than those from controls.

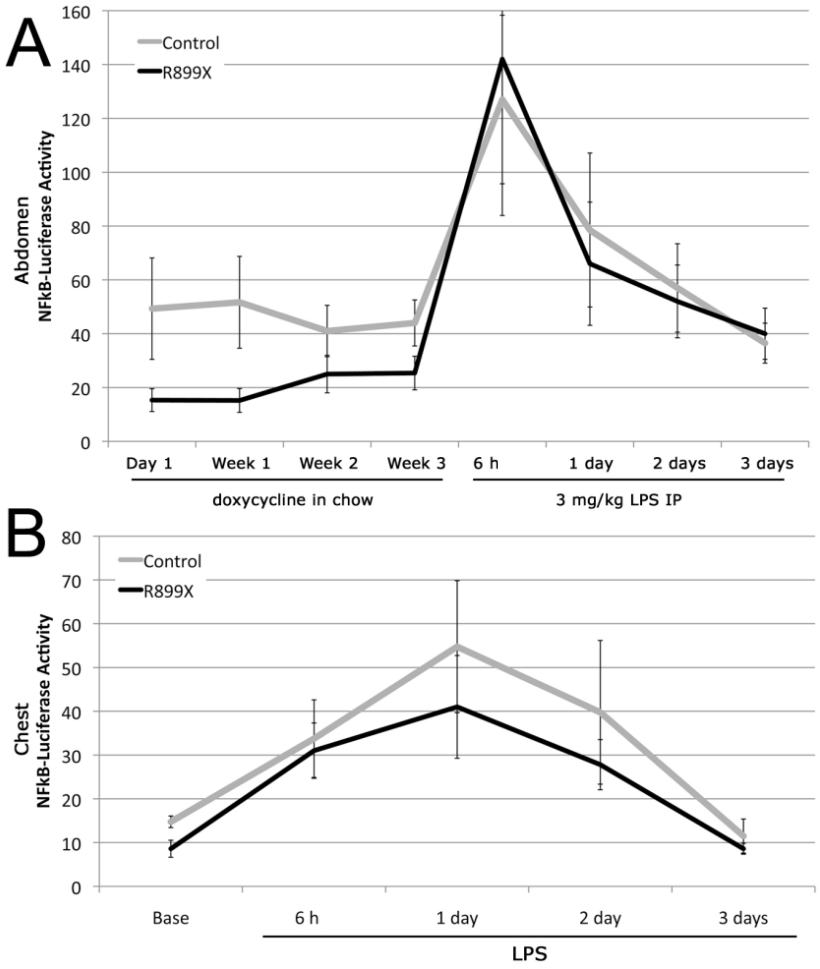

Figure 3. *Cont.*

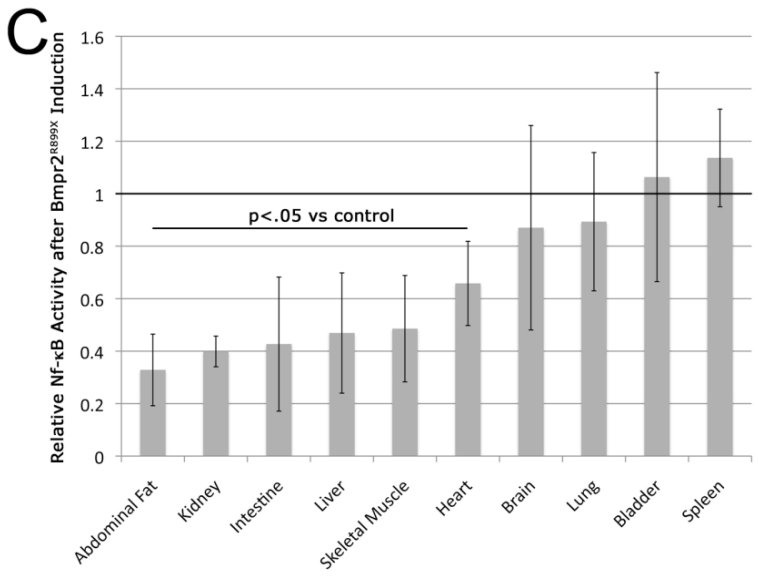

Figure 4. NF-κB activation is not required for murine Bmpr2-related pulmonary arterial hypertension (PAH). (**A**) While Rosa26-Bmpr2^{R899X} mice had significantly higher RVSP compared to controls (p = 0.0005 by Fisher's LSD after two-way ANOVA, p = 0.0017 by Wilcoxon), this was not altered by expression of dnIκB. Each circle corresponds to measurements from one mouse; grey bars are means. (**B**) Smad phosphorylation is not altered by dnIκB or by expression of Bmpr2^{R899X}; densitometry is normalized to beta-actin levels. The Bmpr2^{R899X} has been previously shown to leave Smad signaling intact [10], and so this result was expected. Numbers under each blot are densitometry normalized to beta-actin; the plot at bottom is phosphorylated normalized to total protein. (**C**) Expression of dnIκB produces a trend towards increased muscularization in vessels in the lungs, but it is not statistically significant by two-way ANOVA.

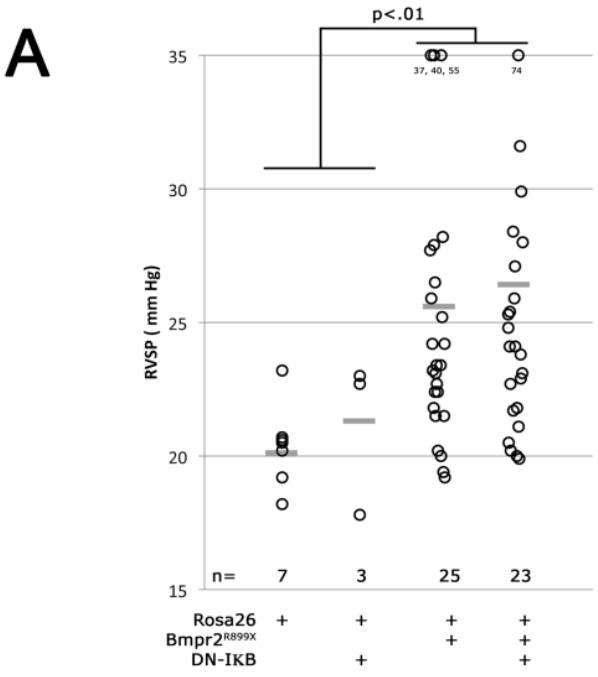

Figure 4. *Cont.*

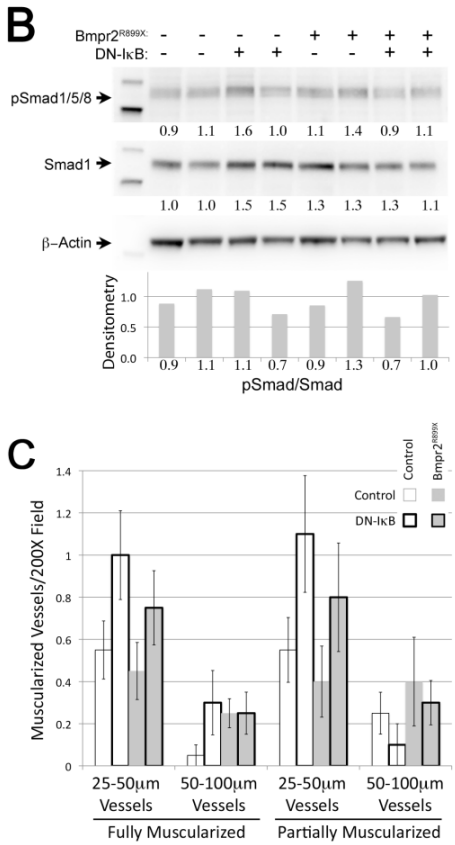

3.5. NF-κB Activation Exacerbates Murine Bmpr2-Related PH

While the previous results indicate NF-κB activation is not required for murine Bmpr2-related PH, NF-κB activation could still contribute. To test this, Rosa26-only or Rosa26-Bmpr2^{R899X} mice had transgene induced for two weeks, then had intratracheal instillation of either empty adenovirus or adenovirus encoding the active NF-κB molecule, RelA [25]. Intratracheal instillation of the RelA virus results in primarily epithelial infection [35,36], and so inflammatory effect on the vasculature was likely a secondary effect. After an additional 4 weeks, after either virus was cleared (quantitative PCR showed no sign of virus in lung or liver, not shown), we performed hemodynamic phenotyping as above.

We found that RelA virus increased average pressure by 4 mm Hg in Rosa26-only control mice and 8 mm Hg in Rosa26-Bmpr2^{R899X} mice (Figure 5A). Cardiac output in control mice with control and RelA adenovirus were the same, averaging 8.8 mL/min and 8.4 mL/min respectively; cardiac output in Rosa26-Bmpr2^{R899X} mice dropped from 8.2 to 6.9 mL/min, reflecting a significant increase in pulmonary vascular resistance (Figure 5B). RelA virus increased PVR by 31% in control mice, and to 220% of control values (an average of 155 dyn*s/cm^5) in Rosa26-Bmpr2^{R899X} mice. Every mutant mouse receiving RelA virus had a PVR of over 100, making measurable disease penetrance 100% by this metric. RelA virus had no impact on other measured variables (weight, blood glucose, *etc.*, not shown), and by the time of sacrifice had no impact on Bmpr2 activity as assessed by Smad phosphorylation (Figure 5C), although based on Figure 2, we expect that it would have had the effect of at least transient suppression of canonical Bmp signaling when first injected.

Figure 5. RelA virus exacerbates pulmonary arterial hypertension in Bmpr2^{R899X} mice. (**A**) By two-way ANOVA, Bmpr2^{R899X} genotype increased RVSP at $p = 0.0042$ and Rel-A virus increased RVSP at $p = 0.03$. Using non-parametric statistics (Wilcoxon) difference between groups is $p = 0.0021$, with rel-A causing a significant increase in RVSP in Bmpr2^{R899X} mice. Each circle corresponds to an individual mouse: grey bars are means. (**B**) By two-way ANOVA, Bmpr2^{R899X} genotype increased pulmonary vascular resistance (PVR) at $p = 0.0078$ and Rel-A virus increased RVSP at $p = 0.0126$. Using non-parametric statistics (Wilcoxon) difference between groups is $p = 0.0020$. (**C**) Neither Rel-A virus nor Bmpr2^{R899X} expression had a significant effect on Smad1 phosphorylation in whole mouse lung. By the time of sacrifice, though, Rel-A virus would have been cleared for at least a week. Numbers under each blot are densitometry normalized to beta-actin; the plot at bottom is phosphorylated normalized to total protein. (**D**) The mechanism of continuing increased RVSP resulting from Rel-A virus is likely through increased pulmonary vascular remodeling. There is a near doubling of partially and fully muscularized 25–50 m vessels in mutant mice receiving Rel-A virus. (**E**) Lung sections stained for smooth muscle actin (green) show a dramatic increase in muscularized small vessels (arrowheads) in Bmpr2^{R899X} expression mice receiving Rel-A virus.

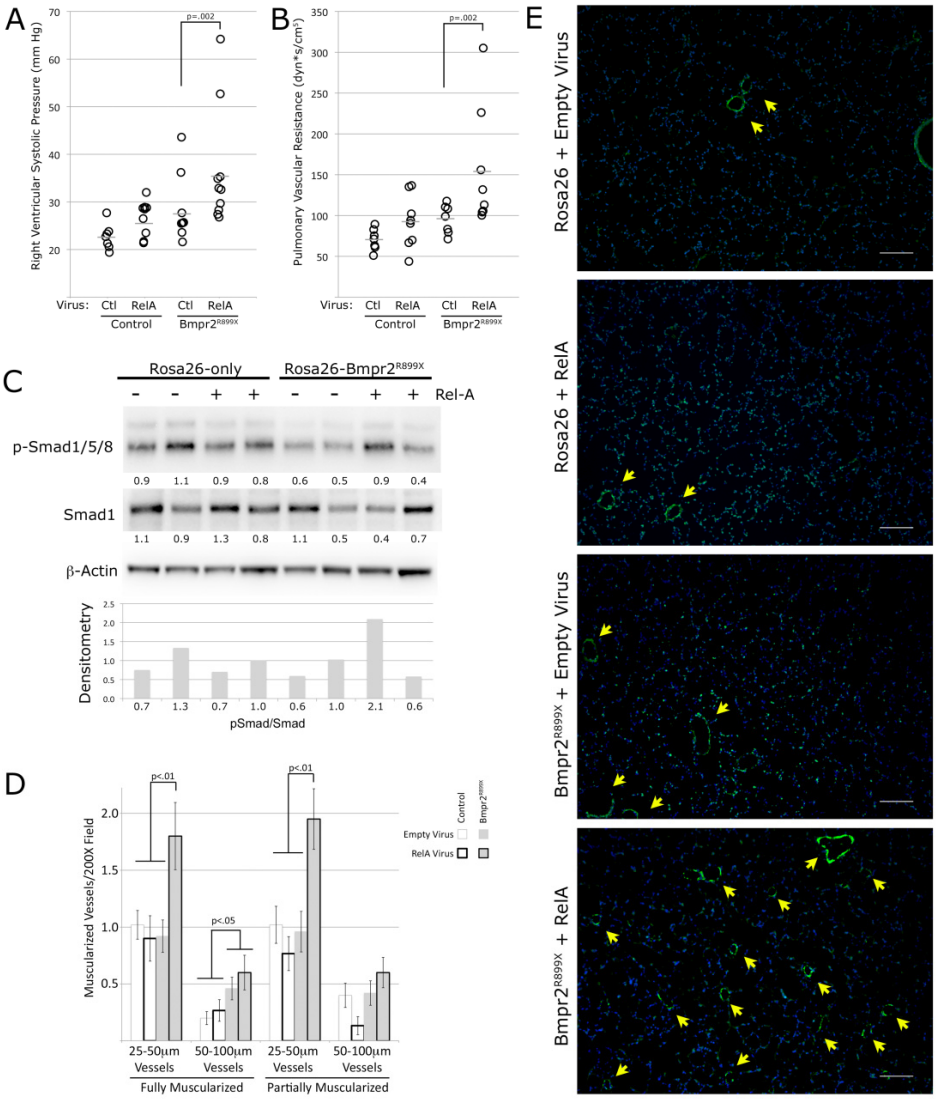

We quantified numbers of fully and partially muscularized vessels of different sizes in 10 random fields from each of 4 mice from each group. We found that Bmpr2 mutant mice that had received RelA virus had near doubling in muscularized small vessels (Figure 5D,E), not found in control mice. This increase in NF-κB driven muscularization is the most likely explanation for the persistent increase in RVSP in $Bmpr2^{R899X}$ mice, long after clearance of the virus.

3.5. Discussion

While inflammation is probably causative in some secondary forms of PAH such as schistosomiasis and sarcoidosis [5], whether or not activation of NF-κB (or any inflammatory pathway) is causative in idiopathic PAH is unknown. NF-κB is activated in end-stage disease in human idiopathic and heritable PAH patients [31]. However, animal models of PH have firmly established that the inflammatory response, including NF-κB activation, are part of the response to high pressure, and mediate phenomena such as increased muscularization of vessels and thickening of adventitia [30,37]. Further, lungs from patients in the Prostacyclin era have substantially worse inflammation than those that were never treated [38], suggesting that perhaps inflammation is an epiphenomenon, or even protective, in human disease. Neither classical animal models nor human data thus clarify the issue of whether NF-κB activation is part of initial pathogenesis.

To study this, we turned to BMPR2 mutant mice. BMPR2 mutation is the cause of roughly 80% of heritable PAH, and it is suppressed in all forms of idiopathic PAH [39–41], with the molecular signature of disease nearly indistinguishable between patients with and without BMPR2 mutation [8]. It is one of the only known direct causes of PH in humans (the other being use of serotonergic drugs). The relationship between NF-κB activation and development of elevated pressure with BMPR2 mutation is thus potentially important for understanding the etiology and possible interventions of most classes of PAH.

The results of this study are summarized in Figure 6, combined with some data from the literature. The effect of NF-κB activation is most straightforward. It is activated in late PH, both in humans and in mice (Figure 1). NF-κB activation worsens disease, probably through increases in muscularization (Figure 5) but also through alteration in the behavior of inflammatory cells [42]. NF-κB activation also suppresses BMP pathway function, either with acute inflammation or with long-term genetic activation (Figure 2), which probably at least partially explains why the BMP pathway is suppressed in all forms of PH in humans. This might explain the common findings of active virus in IPAH [43]. While there has been no consistency in the type of virus found, by this hypothesis, the type of virus is really less important than its presence: Just about any virus will cause NF-B activation and thus suppression of the BMP pathway.

Conversely, we found that Bmpr2 tail domain mutation did not lead directly to NF-κB activation (Figure 3), and in fact was associated with a moderate decrease in some organs. The BMP pathway has been published to regulate NF-κB through X-linked inhibitor of apoptosis [44] mediated by the type I receptor. However, the Bmpr2 mutation used in this study does not affect type I receptor-mediated signaling. Studies using a different Bmpr2 mutation, that does affect type I receptor-mediated signaling, did lead to increased NF-κB activation, but only in circulating cells [42].

Figure 6. This study suggests that BMPR2 activation of NF-κB is indirect, occurring only after pulmonary vascular pressures are already increased (Figures 1, 3 and 4), while NF-κB suppression of BMP signaling is more direct, occurring acutely (Figure 2) and worsening muscularization and pulmonary pressures (Figure 5).

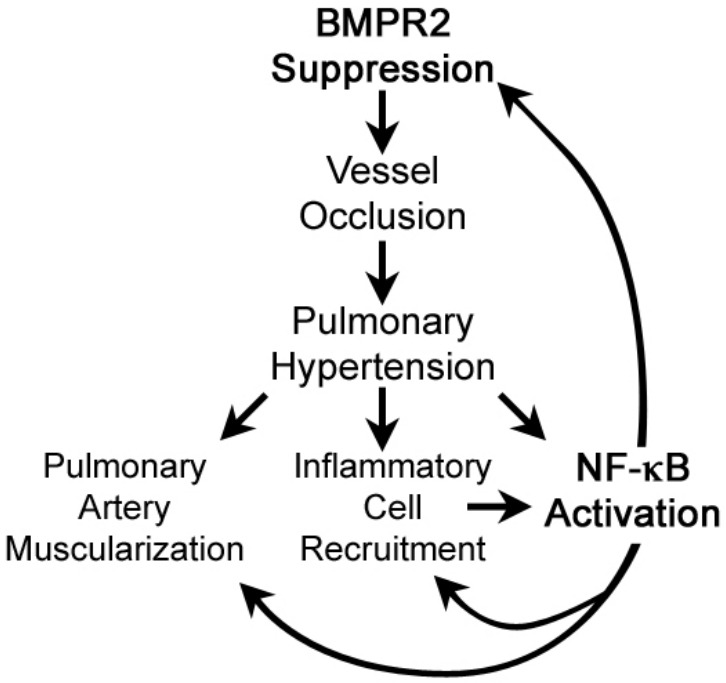

Further, inhibition of NF-B using a dominant negative IB line *in vivo* had no effect, either positive or negative, on RVSP or penetrance in $Bmpr2^{R899X}$ mice (Figure 4), indicating that NF-B-dependent inflammation is not required for Bmpr2-dependent PH.

The technical limitations of this study is, experiments are all done in whole mice or whole tissues, and so we plan to perform more targeted cell specific induction or suppression NF-B activity. Based on histology in Figure 1, it seems likely that the majority of the signal arises from circulating cells. Next, the mouse models all use inducible expression of dominantly negative Bmpr2 or IkB—they thus do not represent normal regulation. For instance, it is possible that for the endogenous genes, suppression of NF-B would result in induction of the BMP pathway. Because our transgenes are not under normal regulation, this would not be possible at the level of transcription in this model. Next, BMPR2 has been shown to regulate NF-B through a mechanism involving TAB1/TAK1 and the type 1 BMP receptor [45]; we explicitly chose to use a BMPR2 mutation which left this signaling intact, since both in mice and in humans mutations affecting this pathway are not required for the development of PH. These technical limitations do not alter our primary conclusions, but do limit their scope.

Perhaps more important are the conceptual limitations: questions that this study does not answer, and was not designed to answer. This study does not show that inflammatory processes or cells are not required for the initiation or progression of Bmpr2-related PH. Human pulmonary arterial hypertension is heavily associated with increased local and circulating cytokines, and, especially in the prostacyclin era, massive recruitment of inflammatory cells to the lungs [14,46–49]. Based on animal models, it seems very likely that this inflammation is a necessary part of remodeling [50], which, although it may not be important in initiation of disease, is probably important in maintenance and progression

of disease, not studied in the current project. Even for initiation of disease in Bmpr2 mutants, it seems very likely that inflammatory processes are required. The current study shows that these processes must not be NF-B dependent, but they could easily be dependent on other inflammatory pathways. For instance, both Stat3 [51] and Stat5 [52] have been linked to PAH, as has the MAPK pathway [53,54], all of which could be operating independently of NF-B.

4. Conclusions

In summary, while NF-κB is activated in end-stage PH, mutation of the cytoplasmic tail domain in Bmpr2 does not directly result in NF-κB activation, and causes suppression of NF-κB in many tissues. The present data support the conclusion that NF-κB activation exacerbates, but is not required for Bmpr2-related PH.

Acknowledgement

The work was funded by RO1 Grants HL82694 and HL095797, the North Carolina Chapter of National Lung Cancer Partnership, and Vanderbilt Allergy, Pulmonary and Critical Care Division internal funds.

Author Contributions

JW: had full access to all of the data in this study and takes responsibility for the integrity of the data and accuracy of the data analysis. JW: Contributed to the study design, data acquisition, analysis, and interpretation, writing and editing the manuscript and served as a principal author. MT and HM: Contributed to the study design, data acquisition, analysis, and interpretation, writing and editing the manuscript. KL, WH and OM: contributed to study design, acquisition, analysis, and interpretation of the data, writing manuscript and approved the final manuscript. Tom B and RZ: contributed to conducting experiments and data anaylsis and approved the final manuscript. AH and Timothy B: contributed to study design; acquisition, analysis, and interpretation of the data; writing and editing the manuscript; and approved the final manuscript.

Conflicts of Interest

The authors declare no conflict of interest.

References

1. Stenmark, K.R.; Meyrick, B.; Galie, N.; Mooi, W.J.; McMurtry, I.F. Animal models of pulmonary arterial hypertension: The hope for etiological discovery and pharmacological cure. *Am. J. Physiol. Lung Cell. Mol. Physiol.* **2009**, *297*, L1013–L1032.
2. Moosmang, S.; Schulla, V.; Welling, A.; Feil, R.; Feil, S.; Wegener, J.W.; Hofmann, F.; Klugbauer, N. Dominant role of smooth muscle L-type calcium channel Cav1.2 for blood pressure regulation. *EMBO J.* **2003**, *22*, 6027–6034.

3. Bonnet, S.; Michelakis, E.D.; Porter, C.J.; Andrade-Navarro, M.A.; Thebaud, B.; Haromy, A.; Harry, G.; Moudgil, R.; McMurtry, M.S.; Weir, E.K.; *et al*. An abnormal mitochondrial-hypoxia inducible factor-1alpha-Kv channel pathway disrupts oxygen sensing and triggers pulmonary arterial hypertension in fawn hooded rats: Similarities to human pulmonary arterial hypertension. *Circulation* **2006**, *113*, 2630–2641.
4. Maurer, B.; Reich, N.; Juengel, A.; Kriegsmann, J.; Gay, R.E.; Schett, G.; Michel, B.A.; Gay, S.; Distler, J.H.; Distler, O. Fra-2 transgenic mice as a novel model of pulmonary hypertension associated with systemic sclerosis. *Ann. Rheum. Dis.* **2012**, *71*, 1382–1387.
5. Crosby, A.; Jones, FM.; Southwood, M.; Stewart, S.; Schermuly, R.; Butrous, G.; Dunne, D.W.; Morrell, N.W. Pulmonary vascular remodeling correlates with lung eggs and cytokines in murine schistosomiasis. *Am. J. Respir. Crit. Care Med.* **2010**, *81*, 279–288.
6. Cogan, J.D.; Vnencak-Jones, C.L.; Phillips, J.A., 3rd.; Lane, K.B.; Wheeler, L.A.; Robbins, I.M.; Garrison, G.; Hedges, L.K.; Loyd, J.E. Gross BMPR2 gene rearrangements constitute a new cause for primary pulmonary hypertension. *Genet. Med.* **2005**, *7*, 169–174.
7. Lane, K.B.; Machado, R.D.; Pauciulo, M.W.; Thomson, J.R.; Phillips, J.A., 3rd.; Loyd, J.E.; Nichols, W.C.; Trembath, R.C. Heterozygous germline mutations in BMPR2, encoding a TGF-beta receptor, cause familial primary pulmonary hypertension. *Nat. Genet.* **2000**, *26*, 81–84.
8. Austin, E.D.; Menon, S.; Hemnes, A.R.; Robinson, L.R.; Talati, M.; Fox, K.L.; Cogan, J.D.; Hamid, R.; Hedges, L.K.; Robbins, I.; *et al*. Idiopathic and heritable PAH perturb common molecular pathways, correlated with increased MSX1 inexpression. *Pulm. Circ.* **2011**, *1*, 389–398.
9. Tada, Y.; Majka, S.; Carr, M.; Harral, J.; Crona, D.; Kuriyama, T.; West, J. Molecular effects of loss of BMPR2 signaling in smooth muscle in a transgenic mouse model of PAH. *Am. J. Physiol. Lung Cell. Mol. Physiol.* **2007**, *292*, L1556–L1563.
10. West, J.; Harral, J.; Lane, K.; Deng, Y.; Ickes, B.; Crona, D.; Albu, S.; Stewart, D.; Fagan, K. Mice expressing BMPR2R899X transgene in smooth muscle develop pulmonary vascular lesions. *Am. J. Physiol. Lung Cell. Mol. Physiol.* **2008**, *295*, L744–L755.
11. Majka, S.; Hagen, M.; Blackwell, T.; Harral, J.; Johnson, J.A.; Gendron, R.; Paradis, H.; Crona, D.; Loyd, J.E.; Nozik-Grayck, E.; *et al*. Physiologic and molecular consequences of endothelial Bmpr2 mutation. *Respir. Res.* **2011**, *12*, 84.
12. Talati, M.; West, J.; Blackwell, T.R.; Loyd, J.E.; Meyrick, B. BMPR2 mutation alters the lung macrophage endothelin-1 cascade in a mouse model and patients with heritable pulmonary artery hypertension. *Am. J. Physiol. Lung Cell. Mol. Physiol.* **2010**, *299*, L363–L373.
13. Hagen, M.; Fagan, K.; Steudel, W.; Carr, M.; Lane, K.; Rodman, D.M.; West, J. Interaction of interleukin-6 and the BMP pathway in pulmonary smooth muscle. *Am. J. Physiol. Lung Cell. Mol. Physiol.* **2007**, *292*, L1473–L1479.
14. Tuder, R.M.; Groves, B.; Badesch, D.B.; Voelkel, N.F. Exuberant endothelial cell growth and elements of inflammation are present in plexiform lesions of pulmonary hypertension. *Am. J. Pathol.* **1994**, *144*, 275–285.
15. Perros, F.; Dorfmuller, P.; Montani, D.; Hammad, H.; Waelput, W.; Girerd, B.; Raymond, N.; Mercier, O.; Mussot, S.; Cohen-Kaminsky, S.; *et al*. Pulmonary lymphoid neogenesis in idiopathic pulmonary arterial hypertension. *Am. J. Respir. Crit. Care Med.* **2012**, *185*, 311–321.

16. Tamosiuniene, R.; Tian, W.; Dhillon, G.; Wang, L.; Sung, Y.K.; Gera, L.; Patterson, A.J.; Agrawal, R.; Rabinovitch, M.; Ambler, K.; *et al*. Regulatory T cells limit vascular endothelial injury and prevent pulmonary hypertension. *Circ. Res.* **2011**, *109*, 867–879.
17. Yu, Y.; Keller, S.H.; Remillard, C.V.; Safrina, O.; Nicholson, A.; Zhang, S.L.; Jiang, W.; Vangala, N.; Landsberg, J.W.; Wang, J.Y.; *et al*. A functional single-nucleotide polymorphism in the TRPC6 gene promoter associated with idiopathic pulmonary arterial hypertension. *Circulation* **2009**, *119*, 2313–2322.
18. Sawada, H.; Saito, T.; Nickel, N.P.; Alastalo, T.P.; Glotzbach, J.P.; Chan, R.; Haghighat, L.; Fuchs, G.; Januszyk, M.; Cao, A.; *et al*. Reduced BMPR2 expression induces GM-CSF translation and macrophage recruitment in humans and mice to exacerbate pulmonary hypertension. *J. Exp. Med.* **2014**, *211*, 263–280.
19. Hayden, M.S.; Ghosh, S. NF-kappaB in immunobiology. *Cell Res.* **2011**, *21*, 223–244.
20. Johnson, J.A.; Hemnes, A.R.; Perrien, D.S.; Schuster, M.; Robinson, L.J.; Gladson, S.; Loibner, H.; Bai, S.; Blackwell, T.R.; Tada, Y.; *et al*. Cytoskeletal defects in Bmpr2-associated pulmonary arterial hypertension. *Am. J. Physiol. Lung Cell. Mol. Physiol.* **2012**, *302*, L474–L484.
21. West, J. Cross talk between Smad, MAPK, and actin in the etiology of pulmonary arterial hypertension. *Adv. Exp. Med. Biol.* **2010**, *661*, 265–278.
22. Rudarakanchana, N.; Flanagan, J.A.; Chen, H.; Upton, P.D.; Machado, R.; Patel, D.; Trembath, R.C.; Morrell, N.W. Functional analysis of bone morphogenetic protein type II receptor mutations underlying primary pulmonary hypertension. *Hum. Mol. Genet.* **2002**, *11*, 1517–1525.
23. Blackwell, T.S.; Blackwell, T.R.; Christman, J.W. Impaired activation of nuclear factor-kappaB in endotoxin-tolerant rats is associated with down-regulation of chemokine gene expression and inhibition of neutrophilic lung inflammation. *J. Immunol.* **1997**, *158*, 5934–5940.
24. Sadikot, R.T.; Jansen, E.D.; Blackwell, T.R.; Zoia, O.; Yull, F.; Christman, J.W.; Blackwell, T.S. High-dose dexamethasone accentuates nuclear factor-kappa b activation in endotoxin-treated mice. *Am. J. Respir. Crit. Care Med.* **2001**, *164*, 873–878.
25. Sadikot, R.T.; Han, W.; Everhart, M.B.; Zoia, O.; Peebles, R.S.; Jansen, E.D.; Yull, F.E.; Christman, J.W.; Blackwell, T.S. Selective I kappa B kinase expression in airway epithelium generates neutrophilic lung inflammation. *J. Immunol.* **2003**, *170*, 1091–1098.
26. Spurney, C.F.; Knoblach, S.; Pistilli, E.E.; Nagaraju, K.; Martin, G.R.; Hoffman, E.P. Dystrophin-deficient cardiomyopathy in mouse: Expression of Nox4 and Lox are associated with fibrosis and altered functional parameters in the heart. *Neuromuscul. Disord.* **2008**, *18*, 371–381.
27. Tanaka, N.; Dalton, N.; Mao, L.; Rockman, H.A.; Peterson, K.L.; Gottshall, K.R.; Hunter, J.J.; Chien, K.R.; Ross, J., Jr. Transthoracic echocardiography in models of cardiac disease in the mouse. *Circulation* **1996**, *94*, 1109–1117.
28. Cheng, D.S.; Han, W.; Chen, S.M.; Sherrill, T.P.; Chont, M.; Park, G.Y.; Sheller, J.R.; Polosukhin, V.V.; Christman, J.W.; Yull, F.E.; *et al*. Airway epithelium controls lung inflammation and injury through the NF-kappa B pathway. *J. Immunol.* **2007**, *178*, 6504–6513.
29. Zaynagetdinov, R.; Stathopoulos, G.T.; Sherrill, T.P.; Cheng, D.S.; McLoed, A.G.; Ausborn, J.A.; Polosukhin, V.V.; Connelly, L.; Zhou, W.; Fingleton, B.; *et al*. Epithelial nuclear factor-kappaB signaling promotes lung carcinogenesis via recruitment of regulatory T lymphocytes. *Oncogene* **2012**, *31*, 3164–3176.

30. Sawada, H.; Mitani, Y.; Maruyama, J.; Jiang, B.H.; Ikeyama, Y.; Dida, F.A.; Yamamoto, H.; Imanaka-Yoshida, K.; Shimpo, H.; Mizoguchi, A.; *et al*. A nuclear factor-kappaB inhibitor pyrrolidine dithiocarbamate ameliorates pulmonary hypertension in rats. *Chest* **2007**, *132*, 1265–1274.
31. Price, L.C.; Caramori, G.; Perros, F.; Meng, C.; Gambaryan, N.; Dorfmuller, P.; Montani, D.; Casolari, P.; Zhu, J.; Dimopoulos, K.; *et al*. Nuclear factor kappa-B is activated in the pulmonary vessels of patients with end-stage idiopathic pulmonary arterial hypertension. *PLoS One* **2013**, *8*, e75415.
32. Bosmann, M.; Russkamp, N.F.; Ward, P.A. Fingerprinting of the TLR4-induced acute inflammatory response. *Exp. Mol. Pathol.* **2012**, *93*, 319–323.
33. West, J.; Gladson, S.; Johnson, J.; Blackwell, T.; Hemnes, A. BMPR2 Mutation Causes Defects in Glucocorticoid Receptor Shuttling. *Am. J. Respir. Crit. Care Med.* **2011**, *183*, A4955.
34. Sorriento, D.; Santulli, G.; Fusco, A.; Anastasio, A.; Trimarco, B.; Iaccarino, G. Intracardiac injection of AdGRK5-NT reduces left ventricular hypertrophy by inhibiting NF-kappaB-dependent hypertrophic gene expression. *Hypertension* **2010**, *56*, 696–704.
35. Muraoka, R.S.; Bushdid, P.B.; Brantley, D.M.; Yull, F.E.; Kerr, L.D. Mesenchymal expression of nuclear factor-kappaB inhibits epithelial growth and branching in the embryonic chick lung. *Dev. Biol.* **2000**, *225*, 322–338.
36. Sadikot, R.T.; Zeng, H.; Joo, M.; Everhart, M.B.; Sherrill, T.P.; Li, B.; Cheng, D.S.; Yull, F.E.; Christman, J.W.; Blackwell, T.S. Targeted immunomodulation of the NF-kappaB pathway in airway epithelium impacts host defense against Pseudomonas aeruginosa. *J. Immunol.* **2006**, *176*, 4923–4930.
37. Ortiz, L.A.; Champion, H.C.; Lasky, J.A.; Gambelli, F.; Gozal, E.; Hoyle, G.W.; Beasley, M.B.; Hyman, A.L.; Friedman, M.; Kadowitz, P.J. Enalapril protects mice from pulmonary hypertension by inhibiting TNF-mediated activation of NF-kappaB and AP-1. *Am. J. Physiol. Lung Cell. Mol. Physiol.* **2002**, *282*, L1209–L1221.
38. Stacher, E.; Graham, B.B.; Hunt, J.M.; Gandjeva, A.; Groshong, S.D.; McLaughlin, V.V.; Jessup, M.; Grizzle, W.E.; Aldred, M.A.; Cool, C.D.; *et al*. Modern age pathology of pulmonary arterial hypertension. *Am. J. Respir. Crit. Care Med.* **2012**, *186*, 261–272.
39. Geraci, M.W.; Moore, M.; Gesell, T.; Yeager, M.E.; Alger, L.; Golpon, H.; Gao, B.; Loyd, J.E.; Tuder, R.M.; Voelkel, N.F. Gene expression patterns in the lungs of patients with primary pulmonary hypertension: A gene microarray analysis. *Circ. Res.* **2001**, *88*, 555–562.
40. Hamid, R.; Cogan, J.D.; Hedges, L.K.; Austin, E.; Phillips, J.A., 3rd.; Newman, J.H.; Loyd, J.E. Penetrance of pulmonary arterial hypertension is modulated by the expression of normal BMPR2 allele. *Hum. Mutat.* **2009**, *30*, 649–654.
41. Cogan, J.; Austin, E.; Hedges, L.; Womack, B.; West, J.; Loyd, J.; Hamid, R. Role of BMPR2 alternative splicing in heritable pulmonary arterial hypertension penetrance. *Circulation* **2012**, *126*, 1907–1916.
42. Talati, M.; West, J.; Zaynagetdinov, R.; Hong, C.C.; Han, W.; Blackwell, T.; Robinson, L.; Blackwell, T.S.; Lane, K. BMP Pathway Regulation of and by Macrophages. *PLoS One* **2014**, *9*, e94119.

43. Cool, C.D.; Voelkel, N.F.; Bull, T. Viral infection and pulmonary hypertension: Is there an association? *Exp. Rev. Respir. Med.* **2011**, *5*, 207–216.
44. Lu, M.; Lin, S.C.; Huang, Y.; Kang, Y.J.; Rich, R.; Lo, Y.C.; Myszka, D.; Han, J.; Wu, H. XIAP induces NF-kappaB activation via the BIR1/TAB1 interaction and BIR1 dimerization. *Mol. Cell Biol*. **2007**, *26*, 689–702.
45. Matluk, N.; Rochira, J.A.; Karaczyn, A.; Adams, T.; Verdi, J.M. A role for NRAGE in NF-kappaB activation through the non-canonical BMP pathway. *BMC Biol.* **2010**, *8*, 7.
46. Humbert, M.; Monti, G.; Brenot, F.; Sitbon, O.; Portier, A.; Grangeot-Keros, L.; Duroux, P.; Galanaud, P.; Simonneau, G.; Emilie, D. Increased interleukin-1 and interleukin-6 serum concentrations in severe primary pulmonary hypertension. *Am. J. Respir. Crit. Care Med.* **1995**, *151*, 1628–1631.
47. Pinto, R.F.; Higuchi Mde, L.; Aiello, V.D. Decreased numbers of T-lymphocytes and predominance of recently recruited macrophages in the walls of peripheral pulmonary arteries from 26 patients with pulmonary hypertension secondary to congenital cardiac shunts. *Cardiovasc. Pathol.* **2004**, *13*, 268–275.
48. Itoh, T.; Nagaya, N.; Ishibashi-Ueda, H.; Kyotani, S.; Oya, H.; Sakamaki, F.; Kimura, H.; Nakanishi, N. Increased plasma monocyte chemoattractant protein-1 level in idiopathic pulmonary arterial hypertension. *Respirology* **2006**, *11*, 158–163.
49. Sanchez, O.; Marcos, E.; Perros, F.; Fadel, E.; Tu, L.; Humbert, M.; Dartevelle, P.; Simonneau, G.; Adnot, S.; Eddahibi, S. Role of endothelium-derived CC chemokine ligand 2 in idiopathic pulmonary arterial hypertension. *Am. J. Respir. Crit. Care Med.* **2007**, *176*, 1041–1047.
50. Steiner, M.K.; Syrkina, O.L.; Kolliputi, N.; Mark, E.J.; Hales, C.A.; Waxman, A.B. Interleukin-6 overexpression induces pulmonary hypertension. *Circ. Res.* **2009**, *104*, 236–244.
51. Courboulin, A.; Barrier, M.; Perreault, T.; Bonnet, P.; Tremblay, V.L.; Paulin, R.; Tremblay, E.; Lambert, C.; Jacob, M.H.; Bonnet, S.N.; *et.al*. Plumbagin reverses proliferation and resistance to apoptosis in experimental PAH. *Eur. Respir. J.* **2012**, *40*, 618–629.
52. Lee, J.E.; Yang, Y.M.; Liang, F.X.; Gough, D.J.; Levy, D.E.; Sehgal, P.B. Nongenomic STAT5-dependent effects on Golgi apparatus and endoplasmic reticulum structure and function. *Am. J. Physiol. Cell Physiol.* **2012**, *302*, C804–C820.
53. Brown, R.D.; Ambler, S.K.; Li, M.; Sullivan, T.M.; Henry, L.N.; Crossno, J.T., Jr.; Long, C.S.; Garrington, T.P.; Stenmark, K.R. MAP kinase kinase kinase-2 (MEKK2) regulates hypertrophic remodeling of the right ventricle in hypoxia-induced pulmonary hypertension. *Am. J. Physiol. Heart Circ. Physiol.* **2013**, *304*, H269–H281.
54. Nasim, M.T.; Ogo, T.; Chowdhury, H.M.; Zhao, L.; Chen, C.N.; Rhodes, C.; Trembath, R.C. BMPR-II deficiency elicits pro-proliferative and anti-apoptotic responses through the activation of TGFbeta-TAK1-MAPK pathways in PAH. *Hum. Mol. Genet.* **2012**, *21*, 2548–2558.